Materials Today Bio 10 (2021) 100109

Contents lists available at ScienceDirect

Materials Today Bio

journal homepage: www.journals.elsevier.com/materials-today-bio

Nanocomposite hyaluronic acid-based hydrogel for the treatment of esophageal fistulas

E. Piantanida [a,h], I. Boškoski [b,c,h], G. Quero [d], C. Gallo [b,c], Y. Zhang [a], C. Fiorillo [b,c], V. Arena [e], G. Costamagna [b,c,**], S. Perretta [f,***], L. De Cola [a,*,g]

[a] Institut de Science et d'Ingénierie Supramoléculaires, CNRS, UMR 7006, Université de Strasbourg, 8 rue Gaspard Monge, 67000 Strasbourg, France
[b] Digestive Endoscopy Unit, Fondazione Policlinico Universitario Agostino Gemelli IRCCS, Largo Agostino Gemelli, 8 00168 Roma, Italy
[c] Centre for Endoscopic Research Therapeutics and Training (CERTT), Catholic University of Rome, Largo Agostino Gemelli, 1 00168, Italy
[d] Digestive Surgery Unit, Fondazione Policlinico Agostino Gemelli, IRCCS, Rome, Italy
[e] Area of Pathology, Department of Woman and Child Health and Public Health, Fondazione Policlinico Universitario Agostino Gemelli IRCCS, Istituto di Anatomia Patologica, Università Cattolica del Sacro Cuore, Largo Agostino Gemelli, 8 00168, Rome, Italy
[f] IRCAD, Strasbourg 1 place del'Hôpital, 67000 Strasbourg, France

ARTICLE INFO

Keywords:
Injectable hydrogel
Hyaluronic acid derivatives
Fistula treatment
Nanocomposite
Minimally invasive surgery

ABSTRACT

Fistulas are abnormal connections between two body parts that can impair the quality of life. The use of biological glues represents the least invasive procedure to fill the fistula; however, it is limited by the need of multiple injections, the persistence of infection and the failure in the treatment of high-output fistulas. We describe herein the use of an injectable nanocomposite hydrogel that is able to form *in situ* a tissue-mimicking matrix as an innovative material for the treatment of esophageal fistulas. Injectable hydrogels that have the dual advantage of being implantable with a minimally invasive approach and of adapting their shape to the target cavity, while the introduction of mesoporous silica nanoparticles opens the possibility of drug/biomolecules delivery.

The hydrogel is based on hyaluronic acid (HA), the crosslinking process occurs at physiological conditions leading to a hydrogel made of >96% by water and with a large-pore micro-architecture. The kinetic profile of the hydrogel formation is studied as a function of HA molecular weight and concentration with the aim of designing a material that is easily injectable with an endoscopic needle, is formed in a time compatible with the surgical procedure and has final mechanical properties suitable for cell proliferation. The *in vivo* experiments (porcine model) on esophageal-cutaneous fistulas, showed improved healing in the animals treated with the hydrogel compared with the control group.

1. Introduction

Gastrointestinal (GI), and in particular, esophageal fistulas (EFs) are defined as a pathological epithelialized communication between the GI tract and the surrounding compartments and/or organs. Associated morbidity and mortality rates are substantial, especially in case of development of septic complications, nutritional deficits, and concomitant comorbidities [1–3]. Medical treatment, including GI rest, parenteral nutrition, and correction of electrolytes impairments is the current gold standard of treatment, with a success rate up to 70% after a mean time of 8 weeks [1,2,4]. Conversely, major surgery (i.e. esophagectomy) is reserved in case of no responsiveness to the conservative treatment. The role of radiology is very important for drainage of EF with infected collections. With the improvement of flexible endoscopic technology, new tools have been introduced for the minimally invasive management of GI fistulas. Among them, the use of biological glues

* Corresponding author.
** Corresponding author.
*** Corresponding author.
E-mail addresses: guido.costamagna@policlinicogemelli.it (G. Costamagna), silvana.perretta@ircad.fr (S. Perretta), luisa.decola@marionegri.it (L. De Cola).
[g] Present address: Istituto di Ricerche Farmacologiche Mario Negri, IRCCS, and University of Milano, Milano Italy.
[h] These authors contributed equally to the work.

https://doi.org/10.1016/j.mtbio.2021.100109
Received 29 December 2020; Received in revised form 4 March 2021; Accepted 9 March 2021
Available online 27 March 2021

gradually increased in the last two decades [5–7]. Their composition, made of fibrinogen and thrombin, stimulate the expression of growth factors that induce the healing of the anatomical defect, while the clot formed after injection is lately reabsorbed after a mean time of two weeks [8,9]. Although the success rate has been reported up to 86.6% [10], the use of biological glues is limited by the uniformity of the techniques described in literature, the need of multiple injections, the persistence of infection and the failure in the treatment of high-output fistulas. These weak points, of such a promising technique, may be mainly related to the physical properties of most biological sealants, namely, the lack of a sufficient viscosity, the absence of an antimicrobial or anti-inflammatory activity and the low adhesiveness. A suitable material for the treatment of fistula is supposed to be characterized by low viscosity during injection, to be able to sustain its own weight after injection, to avoid percolation outside the injection site, and to form *in situ* a soft solid material able to promote the cicatrization process. Some of these properties are often present in hydrogels, three-dimensional polymeric structures able to entrap large amount of water, which upon an appropriate design can be injectable, forming *in situ* a tissue mimicking matrix. For example, the use of a chitosan based hydrogel has been reported to promote the healing of intestinal fistula in a rat model; however daily applications of the material were necessary [11]. In a clinical study, Krause et al. investigated the possibility to use a commercially available injectable polyacrylamide hydrogel in the treatment of vaginal fistula. The proposed material is however used only as a bulking agent to prevent the leak of biological fluids and it is not designed to induce a cicatrization process of the fistula [12]. In the development of injectable hydrogels [13] it is fundamental not only to consider the final mechanical properties of the material but all the kinetic profile of gel formation. The crosslinking process must occur in a time scale compatible with the surgery. If the gelation occurs too fast (e.g. $<$ 5 min) there is the risk of needle clog, if the gelation takes too long (e.g. $>$1 h) the clinical application of the material will not be possible for practical reasons. Each cell type requires a specific range of substrate stiffness to grow, the elastic modulus of the final hydrogel must therefore be within this range. Epithelial cells, involved in the healing processes, for example, proliferate in scaffolds with 1–2 kPa elastic modulus [14]. Furthermore, *in vivo* applications require the material to be deformable without getting damaged.

Hyaluronic Acid (HA) is a glycosaminoglycan present in the human body where its molecular weight (MW) ranges from disaccharide units up to 10^6–10^7 Da polymers [15,16]. High MW HA has the function of space filler in the extracellular matrix (ECM) where it lubricates and hydrates the tissue while having anti-angiogenic, anti-inflammatory and immunosuppressive activity [15,16]. In mammals HA is degraded by the hyaluronidase enzymes with tetra-saccharides as predominant end-products. During the wound healing process, high MW HA is deposited and it binds to fibrinogen, opening up tissues spaces and allowing leukocytes to remove dead tissue, debris and bacteria [15]. The fragmentation of HA during the catabolic pathway generates products with size-specific biological activities. Fragments in the order of 20 kDa induce the synthesis of inflammatory cytokines, the angiogenesis and the endothelial recognition of the injury that stimulates fibroblast proliferation. Oligomers in the 6–20 kDa MW range interact with cell receptors in a monovalent manner allowing multifragment binding and stimulating cell signaling cascades that induce inflammatory gene expression in dendritic cells [15,17]. HA tetra-saccharides inhibit apoptosis and stimulate the expression of heat shock proteins [15]. In solution, HA forms an entangled 3D network whose rate of formation/disruption influence its rheological response. When the material undergoes a high shear (e.g. during injection) the predominance of the rate of entanglement-disruption imparts thinning behavior to the solution [18]. The shear-thinning behavior of HA solution has been exploited, for example, by Mao and coworkers to 3D-print hydrogel scaffolds that after being loaded with stem cells and implanted *in vivo* promoted the neovascularization in damaged tissue [19]. A large number of possible chemical modifications of HA have been reported in literature, the modification targets are the carboxylic group, the hydroxyl group, or less frequently the N-acetyl group [20,21]. The use of HA-based hydrogels for biomedical applications has been recently reviewed [22–24].

Mesoporous silica nanoparticles (MSNs) are characterized by an extraordinarily high surface area-to-mass ratio and have been used for the controlled delivery of cargos ranging from small molecules up to proteins [25–27]. The particles protect the payload from the surrounding environment and control its release improving the pharmacokinetics. Our group has shown that the incorporation of MSNs in a poly(amidoamine) hydrogel can be exploited for the release of a chemokine able to direct the proliferation of mesenchymal stem cells in the material [28].

Herein, we present an injectable nanocomposite hydrogel based on hyaluronic acid (HA) with the aim of filling a model esophageal fistula and of investigating its long-term ability to promote healing. HA is one of the Nature's most versatile and fascinating macromolecules, being an essential component of natural extracellular matrix. The natural role of HA in wound healing, its strong shear thinning behavior and the wide range of possible chemical modifications, motivated us to choose this polymer for the preparation of an injectable hydrogel with application in the treatment of fistula. The hydrogel was optimized testing different HA concentration and molecular weight (MW) of HA to obtain a material that fulfils all the requirements: injection, kinetics of gelation, and mechanical properties of the final material. Mesoporous silica nanoparticles are introduced in the network with the potential function of drug (e.g. anti-inflammatory) and biomolecule (e.g. connective tissue growth factors) delivery system.

2. Materials and methods

2.1. Materials

5 kDa HA (4659 Da Hyaluronic acid sodium salt) was purchased from abcr GmbH, 100 kDa HA (80–100 kDa Hyaluronic acid sodium salt) was purchased from abcr GmbH, 470 kDa HA (intrinsic viscosity 1.02 m^3/kg) and 810 kDa HA (intrinsic viscosity 1.51 m^3/kg) were purchased from CONTIPRO, 1700 kDa HA was purchased from HTL Biotechnology and provided by Qventis GmbH. Dithiothreitol, methacrylic anhydride, tetraethyl orthosilicate (TEOS), cetyltrimethylammonium bromide (CTAB), (3-Mercaptopropyl)trimethoxysilane and Hyaluronidase type IV-S from bovine testes were purchased from Sigma Aldrich. HeLa cells were purchased from ATCC. High glucose DMEM, AlamarBlue®, Phalloidin Alexa Fluor™ 647 and DAPI (4′,6-Diamidino-2-Phenylindole, Dihydrochloride) were purchased from Thermofischer.

2.2. Rheological measures

The rheological measurements were performed with a Thermofisher HAAKE Mars 40 rheometer equipped with a Peltier temperature module. The measuring geometry and the parameter used are specified in each experiment. For the kinetic studies the solution containing all the reagents was placed in the cup of the instrument right after reagent mixture. The measurements are done using a coaxial cylinder geometry and the hydrogel is covered on the top surface with paraffin oil to prevent water evaporation. The linear viscoelastic range of the material was measured right after the end of the kinetic experiments.

In Fig. S1 are reported the viscosity measures of HA with different molecular weight as a function of the shear stress.

2.3. HA methacrylation

To a 1% wt solution of hyaluronic acid (HA) in water, 10 equivalents of methacrylic anhydride were added under stirring in an ice-bath. The pH was adjusted to 8 with NaOH 5 N. The solution is stirred for 24 h in the ice-bath and the pH is periodically adjusted to 8 with NaOH 5 N. The obtained product was precipitated pouring the solution in ethanol. The precipitate was collected and dialyzed (6–8 kDa regenerated cellulose

membrane) for 2 days. The product was freeze-dried for 2 days to give a white powder.

2.4. Mesoporous silica nanoparticle synthesis

60 mg of triethanolamine and 600 mg of cetyltrimethylammonium bromide (CTAB) were dissolved in 20 mL of H_2O and stirred at 350 rpm at 95 °C for 1 h 1.5 mL of tetraethyl orthosilicate (TEOS) where then added drop by drop and the mixture was kept at 95 °C for 1 h. The particles were washed three times by centrifugation in ethanol. The CTAB template was removed refluxing overnight the particles in a solution of ethanol and HCl. The particles were collected by centrifugation (35 krpm, 15 min, 20 °C), washed three times in water/ethanol, and dried under vacuum.

2.5. Mesoporous silica nanoparticles thiol-functionalization

100 mg of Mesoporous Silica Nanoparticles (MSNs) were suspended in 40 mL of ethanol with 75 μL of NH_3 (28% aqueous solution) and 0.6 mmol of (3-Mercaptopropyl)trimethoxysilane and the mixture was stirred overnight at 60 °C. The particles were washed three time in ethanol, collected by centrifugation (35 krpm, 15 min, 20 °C) and then dried under vacuum.

2.6. Characterization of the MSNs

The prepared MSNs are spherical and uniform in size (Fig. S2a, b) with an average diameter of 45 ± 10 nm. Transmission electron microscopy (TEM) imaging showed the presence of pores in the MSNs, (Fig. S2c). The N_2 adsorption/desorption profile (Fig. S2d) is a type IV isotherm with H1 hysteresis loop typical for cylindrical mesopores open at both ends [29]. The MSN surface area is 506.6 ± 1.5 m^2/g with total pore volume of 0.5 cm^3/g and average pore size of 3.8 nm. The presence of a second pore size peak at 6 nm could indicate that the pores are slightly cone-shaped; the pore volume for pores bigger than 10 nm is attributed to the intraparticle space. The ordered structure of the MSNs was characterized by small-angle x-ray scattering (SAXS) (Fig. S2f). The pattern presents a single broad signal at the scatting value of $q = 0.9$ nm^{-1} attributed to the (1 0 0) Bragg peak. The absence of the additional (1 1 0) and (2 0 0) typical Bragg peaks of hexagonally arranged pores indicates the lack of long-range order [30]. The thiol-functionalization of MSN-SH was confirmed both by X-ray photoelectron spectroscopy (XPS) (atomic ratio Si:S = 97:3) and by thermogravimetric analysis (TGA) ($1.1 \cdot 10^{-3}$ mmol of thiol groups for mg of particles corresponding to an atomic ratio Si:S of 95:5) (Fig. S3a-d).

2.7. Nanocomposite HA hydrogel preparation

The hydrogels are prepared starting from a PBS solution of methacrylated hyaluronic acid (Me_HA) in the concentration and MW specified each time. Thalo-functionalized MSN (MSN-SHs) are sonicated to obtain a homogeneous suspension in a small volume of PBS and are added to the Me_HA solution to have a final concentration of MSN of 1 mg/mL. The dithiothreitol crosslinker is dissolved in a small amount of PBS and added to the solution to obtain a molar ration between the thiol groups and the methacrylate groups of Me_HA of 1:1 -the molar concentration of thiols groups (from the crosslinker) is equal to the molar concentration of methacrylate groups (attached to the HA)-.

2.8. In vitro cell culturing

HeLa cells are grown in Dulbecco's Modified Eagle Medium (DMEM) medium and kept in 75 cm^2 culture flasks (Corning Inc., NY, USA) at 37 °C with a controlled atmosphere of 5% CO_2 until reaching 80–85% of confluence. Then, they were washed twice with PBS and treated with trypsin/ ethylenediaminetetraacetic acid (EDTA) solution to detach them from the flask surface. Cells were split every 2–3 days; the medium was changed daily.

2.9. Cell viability study

HEK293 cells were plated at 10000 cell/well in a 96 well plate containing the hydrogel or nothing (control). After 24 h or 48 h, the DMEM was removed and 40 μL of trypsin were added. Cells were collected and centrifuged at 8500 rpm for 8 min. The pellet of cells was resuspended in 50 μL of PBS. 10 μL of cell suspension were mixed with 10 μL of Trypan blue solution (0.4%, from Thermo Fisher) and then 10 μL of the final mixture were counted using the LUNA™ automated cell counter. All the tests were repeated in triplicate.

2.10. Cell fixation and staining

Cells were fixed on top of the hydrogel samples with 4% paraformaldehyde (PFA) for 15 min. Samples were then washed three times with PBS and kept in Triton X-100 (0.1% in PBS) for 10 min and then in 1% bovine serum albumin (BSA) in PBS for 20 min. Cells were stained with Phalloidin Alexa Fluor® 647 for actin staining for 20 min in the dark at room temperature following the manufacturer protocol, then washed three times with PBS. The nuclear region was stained with 4',6-Diamidino-2-Phenylindole (DAPI) (300 nM) for 5 min and then the material was washed again with PBS three times. DAPI was excited at 405 nm, while Phalloidin Alexa Fluor® 647 was excited at 650 nm.

2.11. HA hydrogel degradation kinetics with hyaluronidase

A quantity of 5 mL of HA hydrogel was prepared as described before and incubated at 37 °C for 24 h to ensure the completion of the crosslinking process. Pieces of around 200 mg were weighted and incubated at 37 °C, 5% CO_2 with 2 mL of phosphate buffered saline (PBS), 2.5–10U/mL hyaluronidase enzyme (Hhase), 12.5–50 U/mL Hhase or 25–100 U/mL Hhase. At each measuring time, the weights of three different pieces of gel for each solution were evaluated and the solutions were replaced.

2.12. In vivo experiments

The study was approved by the Ethical Commitee of Università Cattolica del Sacro Cuore di Roma and the Italian Ministry of Health (number: 822/2019-PR). All the procedures were conducted according to the European Community Council directives and the Italian laws on the animal use and care.

2.13. Creation of the fistula model

Under general anesthesia through a right cervicotomy, the cervical esophagus was identified. A convenient spot on the anterolateral cervical esophagus 30 cm from the dental arches was identified by transillumination using the light of the gastroscope. Using a modified Seldinger technique, the esophageal wall was punctured with an introducer needle and a 9-Fr T-tube (Coloplast, Humleb.k, Denmark) was negotiated into the esophageal lumen over a guidewire under endoscopic view. The external part of the catheter was then tunneled subcutaneously in the neck and secured to the skin to prevent dislodgment and migration. The same procedure was performed on both sides of the esophagus.

3. Results and discussion

3.1. Formulation of the nanocomposite hydrogel

In the development of the hyaluronic acid-based hydrogel, the selection of the crosslinking reaction, the thiol-Michael addition, was dictated by the desired reaction kinetics (gelation in few minutes), the possibility to occur at physiological conditions, without the addition of

an initiator and without generating any by-product. This reaction has already been widely exploited for the preparation of HA-based hydrogels for biomedical applications [31–33]. Among the different possible di-thiol molecules, we choose to use dithiothreitol (DTT) as crosslinker because of its high level of water solubility, and because it is considered non-toxic (LD oral, rat = 400 mg/kg). Methacrylated hyaluronic acid (Me_HA) was prepared following the procedure already reported in literature [34,35]. The methacrylation was confirmed by proton nuclear magnetic resonance (^{1}H NMR) and by attenuated total reflectance–Fourier transform infrared (ATR-FTIR) spectroscopy (Fig. S4). The methacrylation degree is expressed as the percentage of HA units in which the hydroxyl group has been converted in a methacrylate group; it is calculated from the ^{1}H NMR spectra, comparing the integral of the peak at 5.98 ppm with the board peak in the range 3–4 ppm. The methacrylation degree for 5 kDa, 100 kDa, 470 kDa and 810 kDa was 100% (i.e. all the hydroxyl groups have been converted in methacrylate groups) while the methacrylation of 1700 kDa gave a batch-to-batch variability with degree between 50% and 100%. Viscosity tests (Fig. S5a) confirmed that the methacrylation process did not significantly reduce the length of HA chains, as observed by other authors [36], and that the introduction of methacrylate groups did not alter the ability of the system to entangle via hydrogen bonding giving an elastic response at high frequency and low shear stress (Fig. S5b and c). The nanocomposite hydrogel is prepared in PBS (pH 7.4, 0.01 M) by the covalent crosslinking of Me_HA with stoichiometric amount of dithiothreitol (DTT) (thiol-Michael reaction) in presence of mesoporous silica nanoparticles (MSN) functionalized on the external surface with thiol groups (Fig. 1). The presence of thiol groups on the outer surface of the MSN is expected to guarantee the covalent linking of the particles to the polymeric structure and to avoid their sedimentation over time.

The incorporation of MSN in hydrogels with the function of structural agents and biomolecule delivery system has been reported by our group [28].

Spherical MSN with homogeneous size were prepared following the procedure reported in literature [37] and functionalized with (3-Mercaptopropyl)trimethoxysilane (Fig. 1a). The MSNs are spherical and uniform in size (Fig. 1b) with an average diameter of 45 ± 10 nm. The materials have been fully characterized, see methods section. The synthesis of the hydrogel occurs at physiological pH and temperature, without releasing any by-product (Fig. S6); the product is a transparent soft solid material (Fig. 1c and d).

In order to select the optimal formulation for the fistula treatment (gelation time in the range 5–60 min, elastic modulus of around 1–2 kPa and high deformability of the final hydrogel), we have investigated the effect of HA molecular weight, its concentration, and the modulation of the kinetics of hydrogel formation and of the final mechanical properties upon incorporation of different amounts of MSNs. The kinetic curves obtained for HA hydrogels prepared using different MWs of HA and concentrations are reported in Fig. 2.

The process of hydrogel formation can be divided in three phases: Phase 1: $t < t_c$, phase 2: $t_c < t < t_p$ and phase 3: $t_p < t < t_f$. Where: t_c is critical time; t_p is percolation time; t_f is final time. During phase 1, the nucleation of aggregates occurs and covalent bonds are formed at constant rate as described by the Smoluchowski model (Fig. S7) [38]. In phase 2, all the samples show a sigmoidal growth of G′, consistent with the Rouse-like percolation that describes the behavior of interconnected polymers [38]. After t_p, the hydrogel obtained from 810 kDa HA at 1% concentration reaches a plateau, indicating that the crosslinking process is completed. All the other samples, on the other side, show a G′ increase between t_p and t_f indicating that a second mode of growth is occurring. This later might be ascribed to the coarsening of interpolymer bonds [38]. The evolution of the viscous modulus G″ over time gives information about the formation of clusters and their connection to the percolating cluster [39]. At time zero, G″ is an indicator of the viscosity of the starting system; at $t > t_0$, an increase of G″ shows either that clusters are being formed and the viscosity of the system is increasing or that ineffective structures (dangling ends and loops) are being formed. On the other side, a decrease in G″ suggests that the clusters are connecting to the network [39]. When G″ reaches a plateau, a balance of the above mentioned events is achieved. The hydrogel obtained from the 100 kDa HA, 2% concentration (Fig. 2a), presents a monotonic increase of G″ over the measurement time. This indicates that clusters are continuously being formed in the system. On the contrary, the hydrogel obtained from 1700 kDa HA at 3% concentration (Fig. 2d), shows after an initial time in which G″ is constant, a monotonic decrease of the viscous modulus. This profile suggests that there are no free clusters in solution and that the system is more likely a single growing network. A third possible case is found in the hydrogel formed from the 470 kDa HA at 2% concentration (Fig. 2b); in this sample, G″ at first increases showing the formation of clusters in solution then it decreases indicating that the clusters are getting incorporated in the network. The G″ maximum is at the percolation time. Fig. 2e and f show the effect of MW and concentration on the time of hydrogel formation and on the final elastic modulus of the material. The effect of increasing the concentration is, in all the samples, an increase on the G′ modulus both of the starting solution and on the final hydrogel. The effect of the MW, on the contrary, is not trivial as reported also by Tabatabai et al. [38] The gel time is significantly decreased

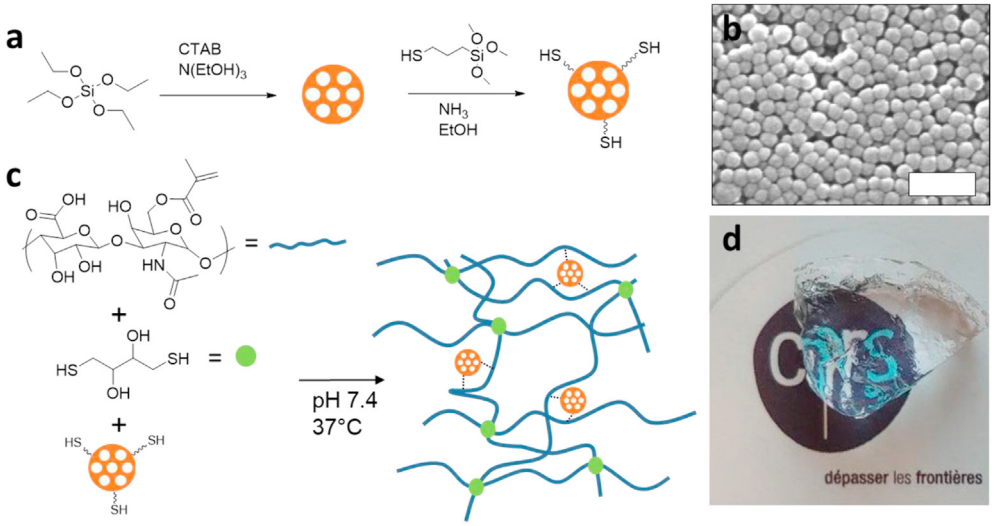

Fig. 1. a) Synthesis of the thiol-functionalized mesoporous silica nanoparticles. b) scanning electron microscopy (SEM) image of the mesoporous silica nanoparticles (scale bar 200 nm). c) Synthesis of the nanocomposite hydrogel. d) The obtained transparent material.

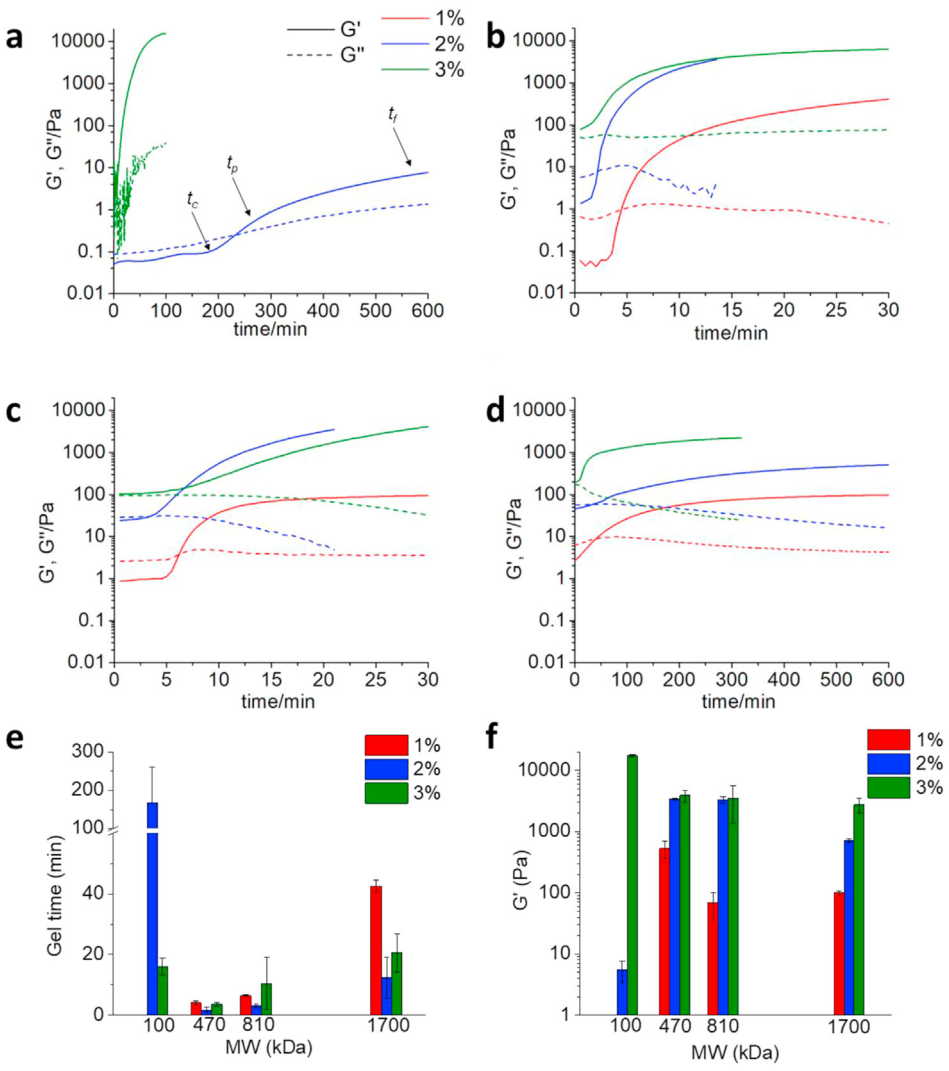

Fig. 2. Kinetics of HA hydrogel formation. 37 °C, $\gamma = 5\%$, $f = 1$ Hz, coaxial cylinder geometry (10 mm). Solid line: G′, dashed line: G″, red line: concentration 1%, blue line: concentration 2%, green line: concentration 3%. a)100 kDa HA, no data are reported for the 1% concentration because the sol-gel transition was not observed in this case. b) 470 kDa HA, c) 810 kDa HA, d) 1700 kDa HA. e) Effect of MW and concentration on the gel time (n = 2); f) effect of MW and concentration on the elastic modulus (n = 2).

passing from 100 kDa HA to 470 kDa HA or 810 kDa HA but it rises again if the MW is increased to 1700 kDa. G′ increases significantly, in the hydrogels obtained at 2% concentration, passing from 100 kDa HA to 470 kDa HA or 810 kDa HA and it decreases again if the MW is increased to 1700 kDa. The polymer's molecular weight (MW) determines the viscosity of the solution before gelation and the number of effective crosslinking reactions required to the formation of a three-dimensional network and a solid hydrogel. Low MW polymers generate lower viscosity solution in which the molecular mobility is higher and the crosslinking reactions are faster. On the other side, low MW polymers require higher number of crosslinking (CL) reactions to obtain a hydrogel while for high MW polymers a smaller number of CL reactions are enough for the formation of the percolating cluster. It is important to underline that the crosslinking reactions can be either effective (e.g. the crosslinking occurs between two different polymeric molecules) or ineffective (intramolecular reactions that bring to the formation of loops) and only the formers contribute to the formation of the 3D network. The hydrogel formation with 100 kDa HA required a very high number of CL reactions, therefore the gelation process is slower and the final material is soft. 1700 kDa HA solutions are characterized by high viscosity that slowdown the reaction process. We hypothesize that the reduction in G' modulus passing from 470 kDa to 1700 kDa HA is due to the higher probability in high MW polymer to have intramolecular ineffective CL reactions.

The ability of the obtained hydrogels to sustain deformation without being damaged can be evaluated by measuring their linear viscoelastic range (LVR). The LVR of all the materials tested mirrors the sample stiffness (Figs. S8 and S9). The LVR of 1700 kDa HA hydrogels is wider (up to $\gamma > 150\%$ at 2% concentration) compared to 470 and 810 kDa ($\gamma < 20\%$, for both at 2% concentration), and this is ascribed to the lower CL degree and to the preservation of the intermolecular mobility. The polymer concentration reduced the LVR in all the samples (Fig. S9). The introduction of thiol-functionalized MSN (MSN-SH) in the hydrogel did not affect either the mechanical properties of the material (Fig. S10a) or the gelation time (Fig. S10b). The observed data are in accordance with literature [40].

By a detailed analysis of all the rheological data and kinetics of formation, for the different MW of HA, and considering that we should mimicking the tissue where the fistula is going to be created, our choice went to 1700 kDa HA. Indeed, such solution before gelation at 3% concentration is characterized by strong shear thinning character that makes it behave as a low viscous fluid during injection and a solid at rest (Fig. S5); the hydrogel is formed in 16 min, the obtained hydrogel has a G' modulus of 2.2 kPa with a wide LVR (up to $\gamma > 30\%$) (Figs. 2 and S8). MSN in concentration 1 mg/mL were moreover introduced in the material to evaluate the possibility to obtain a delivery system, with different release time, that does not perturb the rheological properties of the hydrogels. We evaluated the ability of the solution before preparation of hydrogel (1700 kDa HA, 3%) and of the crosslinked hydrogel to sustain their own weight when deposited on an explanted porcine esophagus and exposed to gravity (Fig. S11). The solution before gelation, owing to its

high viscosity, showed the ability to sustain its own weight and it was maintained after hydrogel formation. The morphological characterization was done by cryo-SEM imaging. This technique, unlike traditional SEM that requires the lyophilization of the sample, allows to observe the pristine structure of the material that conserves the entrapped water (Fig. 3a, b, c, d). The cryo-SEM showed the high porosity of the material with pores in the range 10–50 μm (Fig. 3e). The presence of pores in the size range of cells is of fundamental importance to allow cell proliferation in the material [41] as already shown by Liu et al. with an *in vivo* study. [42] Fig. 3a shows both the pristine frozen sample (bottom left) and the plane where the sample was fractured (top right). Fig. 3b and d are enlargements of the fracture plane showing the ordered pore structure of the sample. The bottom of the pores is filled with ice so it is not possible from these images to estimate the deepness of the pores. The white dots in these pictures are probably ice crystals and not the MSN that are way too small to be observed in these images. Fig. 3c shows an enlargement of the pristine frozen sample where the pores are filled with ice. In Fig. 3f is reported a traditional SEM image of the same sample that underwent the lyophilization process; it is evident that the pores have been enlarged and altered by the freeze-drying process.

3.2. Interaction of epithelial cells with the HA based hydrogel

The cytocompatibility of the developed material was evaluated on human epithelial cells (HEK293). The cells were seeded on the surface of the hydrogel and cultured in presence of culture media. Trypan blue assay indicated that the majority of cells are viable in the material both at 24 h and at 48 h from seeding (Fig. S12). High MW HA (>1000 kDa) is known to inhibit the cellular proliferation [15,16]; however, the presence in mammals of the hyaluronidase enzyme (Hhase) degrades the polymer generating oligomers that have on the contrary the ability to promote cellular adhesion and growth in the material [15]. We investigated the effect of the presence of HA oligomers (5 kDa), in the nanocomposite hydrogel, on the ability of HeLa cells to adhere to the material.

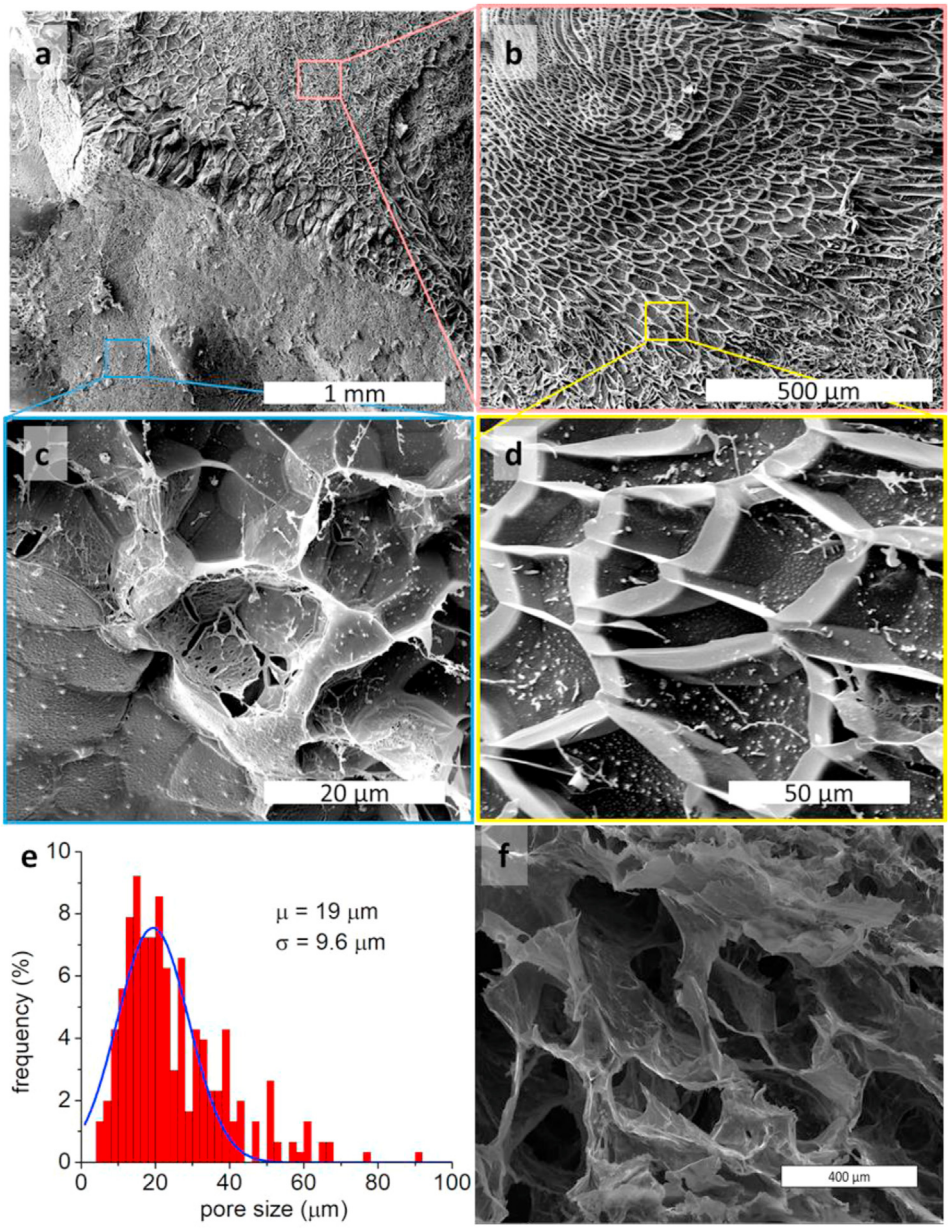

Fig. 3. Cryo-SEM of the nanocomposite hydrogel. a) The top-right part shows the fracture-plane made in the sample. The bottom-left part shows the external surface of the sample. b) Enlargement of the fracture-plane. c) Enlargement of the pristine outer surface of the sample. d) Enlargement of the fracture-plane. e) Pore size distribution obtained from the cryo-SEM images (software *ImageJ*). f) SEM of a lyophilized hydrogel (scale bar 400 μm).

HA hydrogel with different HA oligomer content (5%, 10%, 15%) were prepared and tested for human epithelial cell adhesion (Fig. 4, S13). In absence of oligomers, cells are partially adherent to the hydrogel but they tend to form aggregates and the spreading is reduced (Fig. 4a); the cell spreading was enhanced with the introduction of 5% or 10% oligomers (Fig. 4b and c). A further increase of oligomer concentration (15%) gave the opposite effect with the cells being round shaped and aggregated between each other, probably due to a decrease of the elastic modulus associated to a decrease in the concentration of high molecular weight (MW) hyaluronic acid (HA) polymer (Fig. 4d). These results are of particular interest because they suggest that the *in vivo* application of pure high MW HA hydrogels could give cell adhesion due to the natural presence of hyaluronidase enzyme (Hhase) that generates HA oligomers without the need of introducing integrin-binding peptides.

We evaluated the kinetics of HA hydrogel degradation in presence of different concentrations of Hhase within the human physiological range (from 0.006 U/mL in the plasma to 38.5 U/mL in the ovaries) (Fig. S14) [43]. During the first three days a burst partial mass-loss was observed and it is attributed to the degradation of non-covalently linked HA and/or of dangling ends of the polymer. Indeed, the control experiment using only PBS, showed only a minor mass loss. The enzymatic process then slows down with the hydrogel being completely degraded after more than 30 days. The observed progressive mass loss of the HA hydrogel in presence of Hhase over the 32 days period suggests that the degradation of the material *in vivo* can occur in parallel with the fistula healing process.

3.3. Application of the nanocomposite hydrogel in a porcine model of esophageal fistula

We evaluated the therapeutic effects of the nanocomposite hydrogel in a clinically relevant porcine model of esophageal fistula. The hydrogel

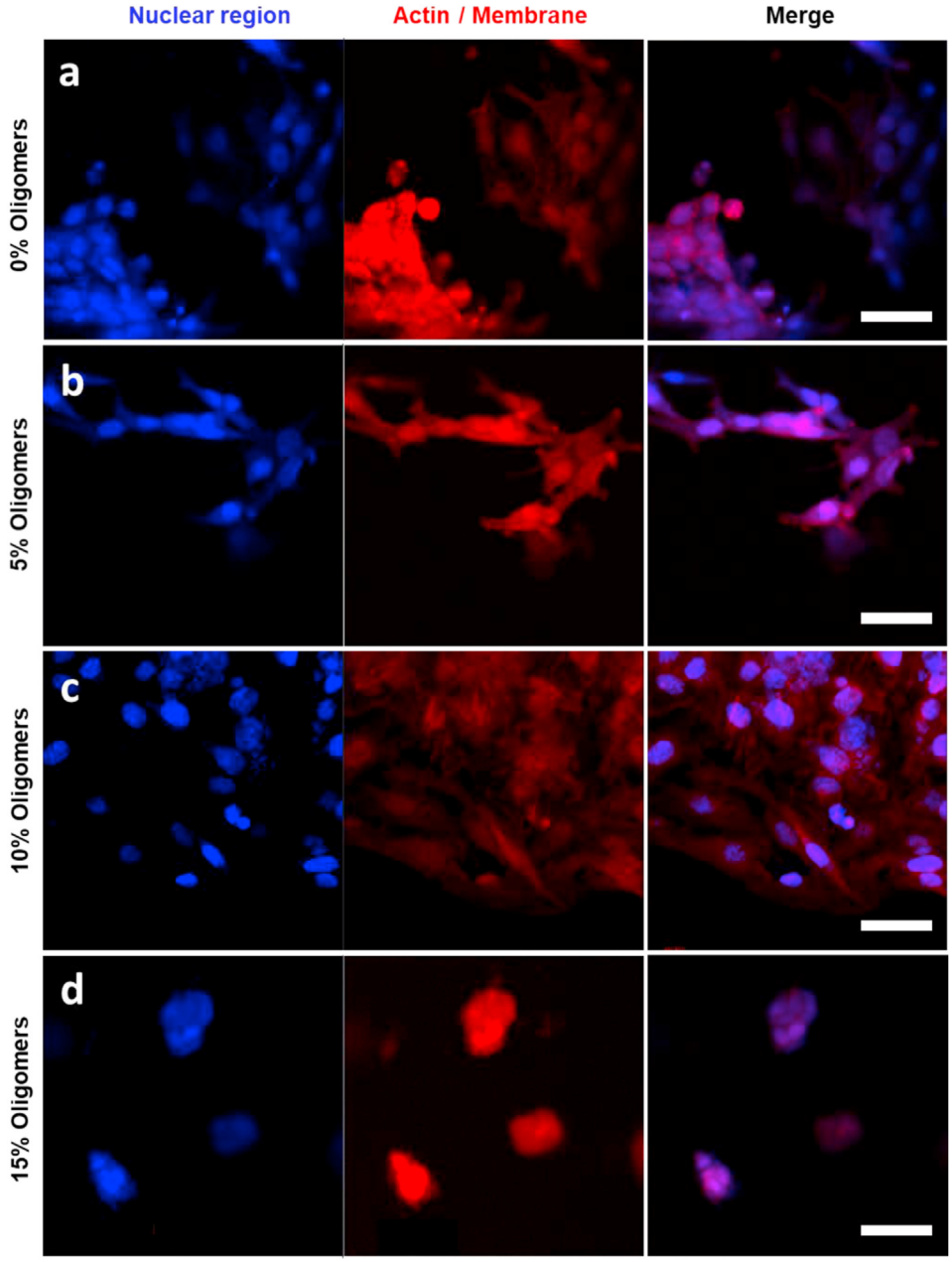

Fig. 4. Confocal imaging of HeLa cells on the surface of HA hydrogels containing a) 0% oligomers, b) 5% oligomers, c) 10% oligomers, d) 15% oligomers. In blue the cellular nucleus stained with DAPI, Actin filaments were labeled with Alexa Fluor®647 Phalloidin. Images in lambda mode. Scale bars: 50 μm

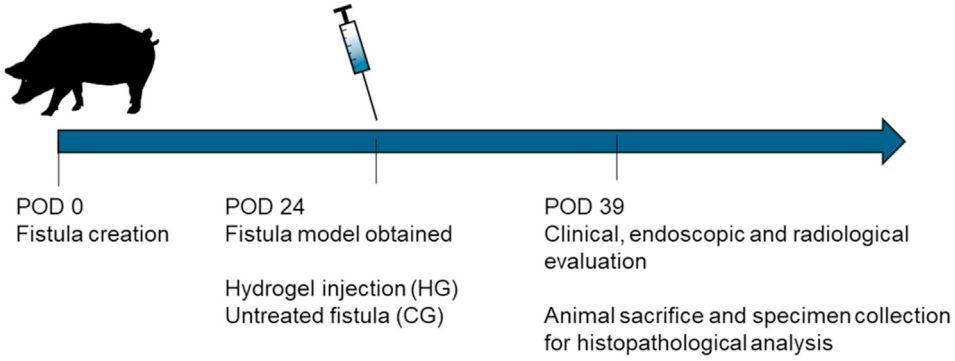

Fig. 5. Time line of the *in vivo* experiment.

precursors were mixed in the surgical room prior of material injection. A total of 4 minipigs (adults, males and females, 35–40 kg) were included in the study. Two esophageal fistulas were created, as previously described [44], for each pig for a total of 8 fistulas obtained at time 0 (post-operative day (POD) 0) (Fig. 5). The animals were kept in the animal facility at the Catholic University of Rome, Italy and they had water and food ad libidum. The animals were fastened the day of the procedure. The process for obtaining a persistent and realistic fistula model last 24 days. The presence and the persistence of the internal and external orifices of the fistulas, was confirmed performing clinical, endoscopic and radiological analysis (at POD 24). Under the clinical point of view, all minipigs maintained a stable weight and did not present any complication after the procedure. Three of the persisting fistulas constituted the control group (CG), while the remaining fistulas (hydrogel filled) constituted the hydrogel group (HG). The CG was untreated, while in the HG a mean value of 6.7 (±3.2) mL of gel was injected in the internal fistula orifice by means of an endoscopic approach (#23 gauge needle). The endoscopic injection process is illustrated in Fig. S15. The complete filling of the cavity with the hydrogel was confirmed by the leaking of a droplet of material from the external fistula orifice.

At POD 39 (corresponding to 15 days after the hydrogel injection), a further clinical, endoscopic, and radiological evaluation was performed (Fig. S16). Macroscopically, in the CG the external fistula orifice was still persistent with a concomitant local inflammation (Fig. 6a). Conversely, in the HG all external fistula orifices were appropriately closed in 5 out of 5 cases (Fig. 6b). The endoscopic re-evaluation similarly demonstrated a persistence of the internal orifice in all the fistulas of the CG (Fig. 6c) and an appropriate closure of the internal orifices in all the fistulas of the HG (Fig. 6d).

After the clinical, endoscopic, and radiological re-evaluation, all minipigs were sacrificed and a specimen for each pig including esophagus, fistula tract and the corresponding muscular, subcutaneous, and cutaneous layers were removed for histopathological analysis (Fig. 7 and S17). In this last regard, a significant inflammatory response was evidenced in the HG with a high concentration of gigantocellular elements, both in the internal and external orifices of the fistulas (Fig. 7a and c). These microscopical aspects demonstrate an appropriate cicatrization

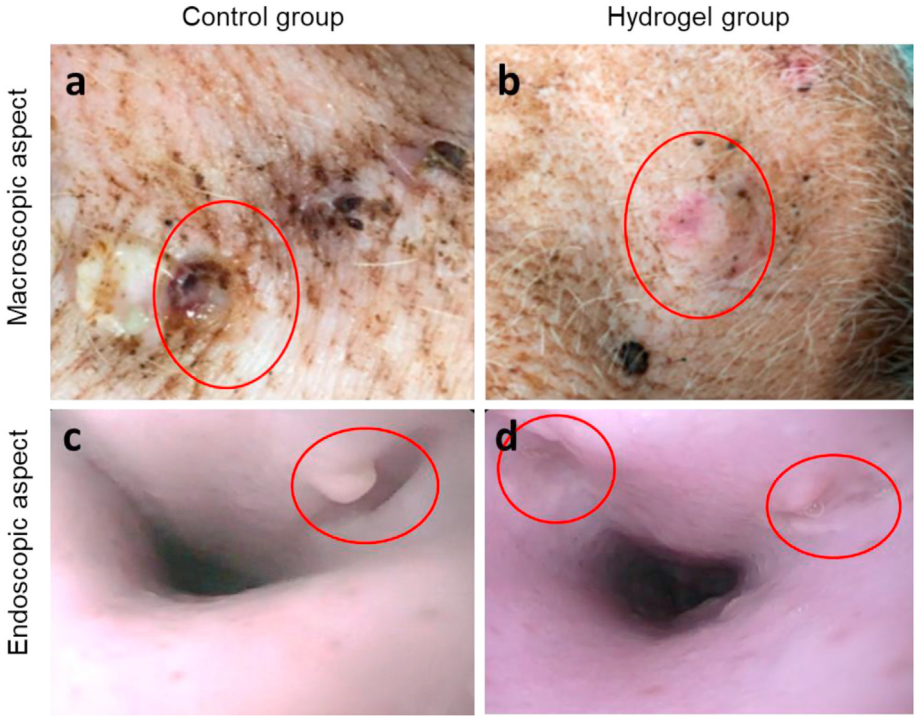

Fig. 6. a, b) Macroscopical aspect of the external orifice of the fistulas (red circles) at time 2 (POD 39): a) persistence and local inflammation in the CG, b) appropriate closure in the HG. c, d) Endoscopic aspect of the internal orifice of the fistulas (red circles) at time 2 (POD 39): c) persistence of the internal orifice in the CG and d) complete closure in the HG.

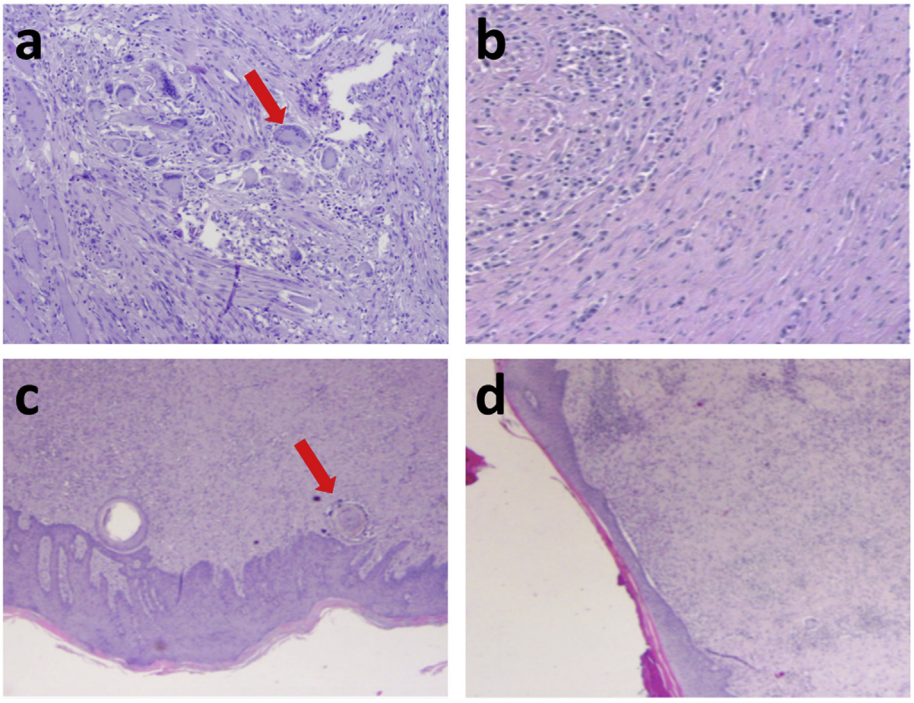

Fig. 7. Histopathological aspect of the a-b) internal (esophageal) and c-d) external (cutaneous) orifices at time 2 (POD 39): inflammatory response with a high concentration of gigantocellular elements (arrow) in the HG (a and c) and aspecific chronic inflammatory response without gigantocellular elements (arrow) in the CG (b and d).

process. Conversely, an aspecific chronic inflammatory response was documented in the CG, both in the internal and external orifices of the fistulas (Fig. 7b and d). The absence of gigantocellular elements microscopically confirms the inappropriate tissue cicatrization process. Based on these macroscopical and microscopical results, we can assume that the injection of hydrogel may induce and accelerate an appropriate healing. The improved cicatrization obtained with the hydrogel suggests that epithelial cells were able to populate the hydrogel. It is possible to hypothesize that the physiologically present hyaluronidase enzyme degraded the injected matrix generating HA oligomers stimulating the cell proliferation (Fig. S14). The degradation of the matrix in parallel with cell growth allows cells to modulate the matrix improving their ability to proliferate and consequently the healing process [45]. The highly porous structure of the material (Fig. 3) is also thought to have played a crucial role in allowing the cell colonization of the hydrogel.

4. Conclusion

A hybrid hyaluronic acid-based hydrogel was designed to be easily injectable, to form *in situ,* in a time compatible with the surgical procedure, and to have mechanical properties able to stimulate the healing process of a fistula. The gelation process occurs at physiological conditions via a thiol-Michael reaction and it gives a large-pore micro-architecture that is thought to play a crucial role in the healing process. *In vitro* tests showed that the incorporation in the hydrogel scaffold of HA oligomers can promote cell adhesion without the need of introducing integrin-binding units. This result is encouraging considering the ability of the naturally present hyaluronidase enzyme to degrade high MW HA generating HA oligomers. Mesoporous silica nanoparticles were introduced in the hydrogel and the material was tested *in vivo* in a clinically relevant porcine model as a filling material for the treatment of esophageal fistula. The hydrogel was easily injectable with an endoscopic needle, after injection it stayed in position without percolating and it formed *in situ* a hydrogel that was completely filling the fistula and promoting cell proliferation and the consequent cicatrization process compared with the control group.

The material obtained is an interesting alternative of the bioglues that are currently used in the treatment of all types of fistula involving the GI tract. The gelation time and the mechanical properties of the proposed hydrogel can be easily adapted to the surgery needs to obtain materials that mimic the target tissue.

Credit author statement

Etienne Piantanida and **Yang Zhang** have synthesized and characterized all the materials and designed some of the experiments.

Ivo Boskoski, Silvana Perretta and Guido Costamagna have designed all the *in vivo* experiments and performed some of the surgery.

Giuseppe Quero, Camilla Gallo, Claudio Fiorillo Vincenzo Arena have done the *in vivo* experiments and the histology on the tissues.

Luisa De Cola has developed the concept and supervised the work.

EP, IB, and LDC have written the paper. All the authors have read and corrected the paper.

Funding

This work was supported by USIAS and Solvay.

Declaration of competing interest

The authors declare that they have no known competing financial interests or personal relationships that could have appeared to influence the work reported in this paper.

Acknowledgements

L.D.C, S.P. and Y.Z. thank USIAS for financial support. E.P. acknowledges Solvay for the Ph.D fellowship. We thank Pierre Picchetti (University of Strasbourg) for the N_2 adsorption, SAXS and TEM analysis, Dr. Laura Talamini (University of Strasbourg) for the cytocompatibility experiments, Dr. Victor Sebastian (University of Zaragoza) for the cryo-SEM imaging and Fabio Longo for the technical support.

Etienne Piantanida and Ivo Boskoski contributed equally to this work.

Appendix A. Supplementary data

Supplementary data to this article can be found online at https://doi.org/10.1016/j.mtbio.2021.100109.

References

[1] A.R. Evenson, J.E. Fischer, Current management of enterocutaneous fistula, J. Gastrointest. Surg. 10 (2006) 455–464, https://doi.org/10.1016/j.gassur.2005.08.001.

[2] P.B. McIntyre, J.K. Ritchie, P.R. Hawley, C.I. Bartram, J.E. Lennard-Jones, Management of enterocutaneous fistulas: a review of 132 cases, Br. J. Surg. 71 (1984) 293–296, https://doi.org/10.1002/bjs.1800710416.

[3] J. Rubelowsky, G.W. Machiedo, Reoperative versus conservative management for gastrointestinal fistulas, Surg. Clin. North Am. 71 (1991) 147–157, https://doi.org/10.1016/s0039-6109(16)45339-9.

[4] G. Dorta, Role of octreotide and somatostatin in the treatment of intestinal fistulae, DIG 60 (1999) 53–56, https://doi.org/10.1159/000051481.

[5] M.K. Goenka, U. Goenka, Endotherapy of leaks and fistula, World J. Gastrointest. Endosc. 7 (2015) 702–713, https://doi.org/10.4253/wjge.v7.i7.702.

[6] P. Rogalski, J. Daniluk, A. Baniukiewicz, E. Wroblewski, A. Dabrowski, Endoscopic management of gastrointestinal perforations, leaks and fistulas, World J. Gastroenterol. 21 (2015) 10542–10552, https://doi.org/10.3748/wjg.v21.i37.10542.

[7] K. Kotzampassi, E. Eleftheriadis, Tissue sealants in endoscopic applications for anastomotic leakage during a 25-year period, Surgery 157 (2015) 79–86, https://doi.org/10.1016/j.surg.2014.06.002.

[8] J.C. Becker, M. Beckbauer, W. Domschke, H. Herbst, T. Pohle, Fibrin glue, healing of gastric mucosal injury, and expression of growth factors: results from a human in vivo study, Gastrointest. Endosc. 61 (2005) 560–567, https://doi.org/10.1016/s0016-5107(05)00291-9.

[9] A. Mizuki, M. Tatemichi, H. Nishiya, K. Fukui, T. Hayashi, N. Tsukada, H. Nagata, H. Ishii, Mucosal concentration of basic fibroblast growth factor in the healing process in human giant gastric ulcers, J. Gastroenterol. Hepatol. 19 (2004) 528–534, https://doi.org/10.1111/j.1440-1746.2004.03359.x.

[10] L.R. Rábago, N. Ventosa, J.L. Castro, J. Marco, N. Herrera, F. Gea, Endoscopic treatment of postoperative fistulas resistant to conservative management using biological fibrin glue, Endoscopy 34 (2002) 632–638, https://doi.org/10.1055/s-2002-33237.

[11] S. Rabbani, A. Rabbani, M.A. Mohagheghi, H. Mirzadeh, S. Amanpour, A. Alibakhshi, M.S. Anvari, Y. Ghazizadeh, A novel approach for repairing of intestinal fistula using chitosan hydrogel, J. Biomater. Appl. 24 (2010) 545–553, https://doi.org/10.1177/0885328208100667.

[12] H.G. Krause, J.P. Lussy, J.T.W. Goh, Use of periurethral injections of polyacrylamide hydrogel for treating post-vesicovaginal fistula closure urinary stress incontinence, J. Obstet. Gynaecol. Res. 40 (2014) 521–525, https://doi.org/10.1111/jog.12176.

[13] E. Piantanida, G. Alonci, A. Bertucci, L. De Cola, Design of nanocomposite injectable hydrogels for minimally invasive surgery, Acc. Chem. Res. 52 (2019) 2101–2112, https://doi.org/10.1021/acs.accounts.9b00114.

[14] D.T. Butcher, T. Alliston, V.M. Weaver, A tense situation: forcing tumour progression, Nat. Rev. Canc. 9 (2009) 108–122, https://doi.org/10.1038/nrc2544.

[15] R. Stern, Hyaluronan catabolism: a new metabolic pathway, Eur. J. Cell Biol. 83 (2004) 317–325, https://doi.org/10.1078/0171-9335-00392.

[16] J.R.E. Fraser, T.C. Laurent, U.B.G. Laurent, Hyaluronan: its nature, distribution, functions and turnover, J. Intern. Med. 242 (1997) 27–33, https://doi.org/10.1046/j.1365-2796.1997.00170.x.

[17] S. Ibrahim, Q.K. Kang, A. Ramamurthi, The impact of HA oligomer content on physical, mechanical, and biologic properties of divinyl sulfone-crosslinked HA hydrogels, J. Biomed. Mater. Res. A 94 (2010) 355–370, https://doi.org/10.1002/jbm.a.32704.

[18] L. Ambrosio, A. Borzacchiello, P.A. Netti, L. Nicolais, Rheological study on hyaluronic acid and its derivative solutions, J. Macromol. Sci., Part A. 36 (1999) 991–1000, https://doi.org/10.1080/10601329908951195.

[19] G. An, F. Guo, X. Liu, Z. Wang, Y. Zhu, Y. Fan, C. Xuan, Y. Li, H. Wu, X. Shi, C. Mao, Functional reconstruction of injured corpus cavernosa using 3D-printed hydrogel scaffolds seeded with HIF-1α-expressing stem cells, Nat. Commun. 11 (2020) 2687, https://doi.org/10.1038/s41467-020-16192-x.

[20] M.A. Serban, A. Skardal, Hyaluronan chemistries for three-dimensional matrix applications, Matrix Biol. 78–79 (2019) 337–345, https://doi.org/10.1016/j.matbio.2018.02.010.

[21] S. Tiwari, P. Bahadur, Modified hyaluronic acid based materials for biomedical applications, Int. J. Biol. Macromol. 121 (2019) 556–571, https://doi.org/10.1016/j.ijbiomac.2018.10.049.

[22] H. Knopf-Marques, M. Pravda, L. Wolfova, V. Velebny, P. Schaaf, N.E. Vrana, P. Lavalle, Hyaluronic acid and its derivatives in coating and delivery systems: applications in tissue engineering, regenerative medicine and immunomodulation, Adv. Healthc. Mater. 5 (2016) 2841–2855, https://doi.org/10.1002/adhm.201600316.

[23] M.F.P. Graça, S.P. Miguel, C.S.D. Cabral, I.J. Correia, Hyaluronic acid—based wound dressings: a review, Carbohydr. Polym. 241 (2020) 116364, https://doi.org/10.1016/j.carbpol.2020.116364.

[24] P. Zhai, X. Peng, B. Li, Y. Liu, H. Sun, X. Li, The application of hyaluronic acid in bone regeneration, Int. J. Biol. Macromol. 151 (2020) 1224–1239, https://doi.org/10.1016/j.ijbiomac.2019.10.169.

[25] Y. Gao, Y. Chen, X. Ji, X. He, Q. Yin, Z. Zhang, J. Shi, Y. Li, Controlled intracellular release of doxorubicin in multidrug-resistant cancer cells by tuning the shell-pore sizes of mesoporous silica nanoparticles, ACS Nano 5 (2011) 9788–9798, https://doi.org/10.1021/nn2033105.

[26] I.I. Slowing, B.G. Trewyn, V.S.-Y. Lin, Mesoporous silica nanoparticles for intracellular delivery of membrane-impermeable proteins, J. Am. Chem. Soc. 129 (2007) 8845–8849, https://doi.org/10.1021/ja0719780.

[27] S. Barui, V. Cauda, Multimodal decorations of mesoporous silica nanoparticles for improved cancer therapy, Pharmaceutics 12 (2020) 527, https://doi.org/10.3390/pharmaceutics12060527.

[28] F. Fiorini, E.A. Prasetyanto, F. Taraballi, L. Pandolfi, F. Monroy, I. López-Montero, E. Tasciotti, L. De Cola, Nanocomposite hydrogels as platform for cells growth, proliferation, and chemotaxis, Small 12 (2016) 4881–4893, https://doi.org/10.1002/smll.201601017.

[29] G. Berlier, L. Gastaldi, E. Ugazio, I. Miletto, P. Iliade, S. Sapino, Stabilization of quercetin flavonoid in MCM-41 mesoporous silica: positive effect of surface functionalization, J. Colloid Interface Sci. 393 (2013) 109–118, https://doi.org/10.1016/j.jcis.2012.10.073.

[30] J.S. Beck, J.C. Vartuli, W.J. Roth, M.E. Leonowicz, C.T. Kresge, K.D. Schmitt, C.T.W. Chu, D.H. Olson, E.W. Sheppard, S.B. McCullen, J.B. Higgins, J.L. Schlenker, A new family of mesoporous molecular sieves prepared with liquid crystal templates, J. Am. Chem. Soc. 114 (1992) 10834–10843, https://doi.org/10.1021/ja00053a020.

[31] J. Kim, Y. Park, G. Tae, K.B. Lee, C.M. Hwang, S.J. Hwang, I.S. Kim, I. Noh, K. Sun, Characterization of low-molecular-weight hyaluronic acid-based hydrogel and differential stem cell responses in the hydrogel microenvironments, J. Biomed. Mater. Res. A 88A (2009) 967–975, https://doi.org/10.1002/jbm.a.31947.

[32] X. Li, B. Cho, R. Martin, M. Seu, C. Zhang, Z. Zhou, J.S. Choi, X. Jiang, L. Chen, G. Walia, J. Yan, M. Callanan, H. Liu, K. Colbert, J. Morrissette-McAlmon, W. Grayson, S. Reddy, J.M. Sacks, H.-Q. Mao, Nanofiber-hydrogel composite–mediated angiogenesis for soft tissue reconstruction, Sci. Transl. Med. 11 (2019), eaau6210, https://doi.org/10.1126/scitranslmed.aau6210.

[33] M.M. Pérez-Madrigal, J.E. Shaw, M.C. Arno, J.A. Hoyland, S.M. Richardson, A.P. Dove, Robust alginate/hyaluronic acid thiol–yne click-hydrogel scaffolds with superior mechanical performance and stability for load-bearing soft tissue engineering, Biomater. Sci. 8 (2020) 405–412, https://doi.org/10.1039/C9BM01494B.

[34] K.A. Smeds, A. Pfister-Serres, D. Miki, K. Dastgheib, M. Inoue, D.L. Hatchell, M.W. Grinstaff, Photocrosslinkable polysaccharides for in situ hydrogel formation, J. Biomed. Mater. Res. 55 (2001) 254–255, https://doi.org/10.1002/1097-4636(200105)55:2<254::AID-JBM1012>3.0.CO;2-5.

[35] J. Yeh, Y. Ling, J.M. Karp, J. Gantz, A. Chandawarkar, G. Eng, J. Blumling III, R. Langer, A. Khademhosseini, Micromolding of shape-controlled, harvestable cell-laden hydrogels, Biomaterials 27 (2006) 5391–5398, https://doi.org/10.1016/j.biomaterials.2006.06.005.

[36] C.E. Schanté, G. Zuber, C. Herlin, T.F. Vandamme, Chemical modifications of hyaluronic acid for the synthesis of derivatives for a broad range of biomedical applications, Carbohydr. Polym. 85 (2011) 469–489, https://doi.org/10.1016/j.carbpol.2011.03.019.

[37] X. Lv, L. Zhang, F. Xing, H. Lin, Controlled synthesis of monodispersed mesoporous silica nanoparticles: particle size tuning and formation mechanism investigation, Microporous Mesoporous Mater. 225 (2016) 238–244, https://doi.org/10.1016/j.micromeso.2015.12.024.

[38] A.P. Tabatabai, B.P. Partlow, N.R. Raia, D.L. Kaplan, D.L. Blair, Silk molecular weight influences the kinetics of enzymatically cross-linked silk hydrogel formation, Langmuir 34 (2018) 15383–15387, https://doi.org/10.1021/acs.langmuir.8b02950.

[39] V. Adibnia, R.J. Hill, Universal aspects of hydrogel gelation kinetics, percolation and viscoelasticity from PA-hydrogel rheology, J. Rheol. 60 (2016) 541–548, https://doi.org/10.1122/1.4948428.

[40] J. Lewandowska-Łańcucka, A. Gilarska, A. Buła, W. Horak, A. Łatkiewicz, M. Nowakowska, Genipin crosslinked bioactive collagen/chitosan/hyaluronic acid injectable hydrogels structurally amended via covalent attachment of surface-modified silica particles, Int. J. Biol. Macromol. 136 (2019) 1196–1208, https://doi.org/10.1016/j.ijbiomac.2019.06.184.

[41] J. Lam, N.F. Truong, T. Segura, Design of cell–matrix interactions in hyaluronic acid hydrogel scaffolds, Acta Biomater. 10 (2014) 1571–1580, https://doi.org/10.1016/j.actbio.2013.07.025.

[42] Y. Liu, X.Z. Shu, G.D. Prestwich, Osteochondral defect repair with autologous bone marrow–derived mesenchymal stem cells in an injectable, *in situ* , cross-linked synthetic extracellular matrix, Tissue Eng. 12 (2006) 3405–3416, https://doi.org/10.1089/ten.2006.12.3405.

[43] Y. Yeo, C.B. Highley, E. Bellas, T. Ito, R. Marini, R. Langer, D.S. Kohane, In situ cross-linkable hyaluronic acid hydrogels prevent post-operative abdominal adhesions in a rabbit model, Biomaterials 27 (2006) 4698–4705, https://doi.org/10.1016/j.biomaterials.2006.04.043.

[44] G. Rahmi, S. Perretta, L. Pidial, G. Vanbiervliet, P. Halvax, A. Legner, V. Lindner, M. Barthet, B. Dallemagne, C. Cellier, O. Clément, A newly designed enterocutaneous esophageal fistula model in the pig, Surg. Innovat. 23 (2016) 221–228, https://doi.org/10.1177/1553350616639144.

[45] S. Khetan, M. Guvendiren, W.R. Legant, D.M. Cohen, C.S. Chen, J.A. Burdick, Degradation-mediated cellular traction directs stem cell fate in covalently crosslinked three-dimensional hydrogels, Nat. Mater. 12 (2013) 458–465, https://doi.org/10.1038/nmat3586.